SUPPLEMENTAL DATA

Kinetics of early TCR signaling regulate the pathway of lytic granule delivery to the secretory domain

Allison M. Beal, Nadia Anikeeva, Rajat Varma, Thomas O. Cameron, Gaia Vasiliver-Shamis, Philip J. Norris, Michael L. Dustin, Yuri Sykulev

Supplemental Results

Faster kinetics of granule delivery is associated with more rapid target cell destruction by CTL

To test whether the difference in the kinetics of granule release could influence the dynamics of target cell killing by CTL, we assessed target cell lysis by more ($CD8^+$) and less ($CD4^+$) effective CTL under conditions when CTL were limited (low effector-to-target ratio). Target cells were sensitized at a peptide concentration required for both CTL to release equal amount of granules (Beal et al., 2008). While $CD8^+$ CTL approached the maximal specific lysis of target cells after 24 hours, $CD4^+$ CTL have only approached 50% of the maximal response by this time (**Fig. S14A**). Consistent with this, we found that $CD8^+$ CTL killing is impaired against target cells sensitized by a weak agonist peptide when CTL numbers are limited (**Fig. S14B**). These data show that more efficient CTL can lyse the same number of same target cells more rapidly than less efficient CTL.

Supplemental Figures

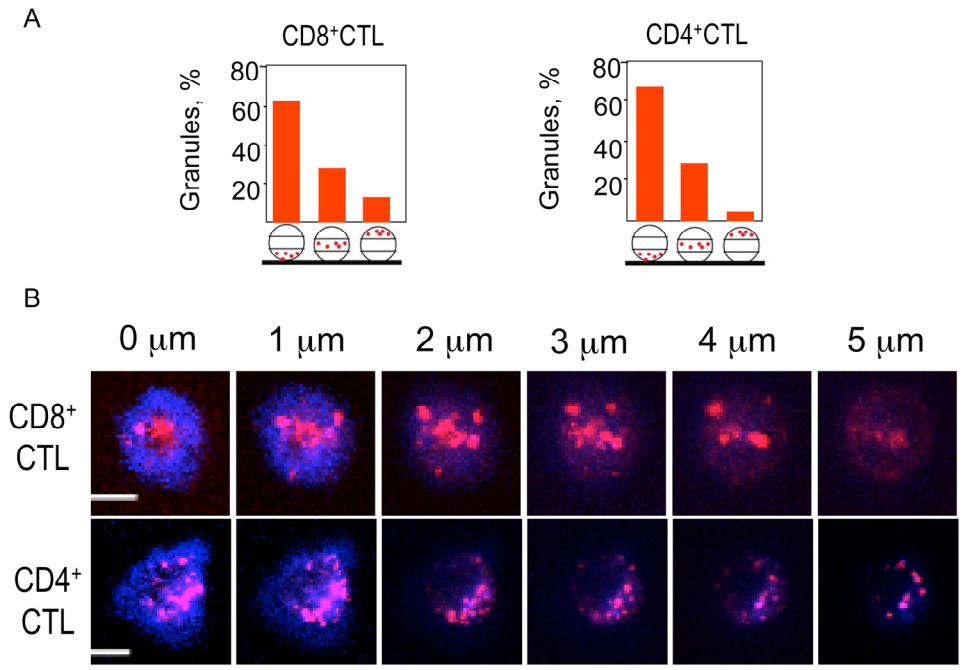

Figure S1. Both $CD8^+$ and $CD4^+$ CTL polarize lytic granules towards the lipid bilayer

(**A**) The average percent of the granules in the lower, middle, and upper thirds of CTL exposed to bilayers loaded with cognate pMHC and ICAM-1 is shown for $CD8^+$ CER43 (left) and $CD4^+$ AC25 (right) CTL. Left diagram was adopted from (Anikeeva et al., 2005). To quantify the distribution of the cytolytic granules, serial axial (z) sections were acquired at 1-μm intervals through the volume of the cells as described previously (Anikeeva et al., 2005). Every cell was then divided into three equal parts along the z-axis starting from the bilayer interface, i.e., bottom, middle and top. Granules in z-sections were quantified based on groups of bright granule pixels and the percentage of granules in each third of the cells was then calculated. (**B**) Representative images of granule distribution in $CD8^+$ (top) and $CD4^+$ (bottom) CTL are shown. The images were

acquired beginning at the bilayer level (0 μm) and going up by 1 μm increments along the Z-axis through the entire cell, but only the first 6 sections are shown. ICAM-1 is blue and granules are red. Scale bar: 5 μm.

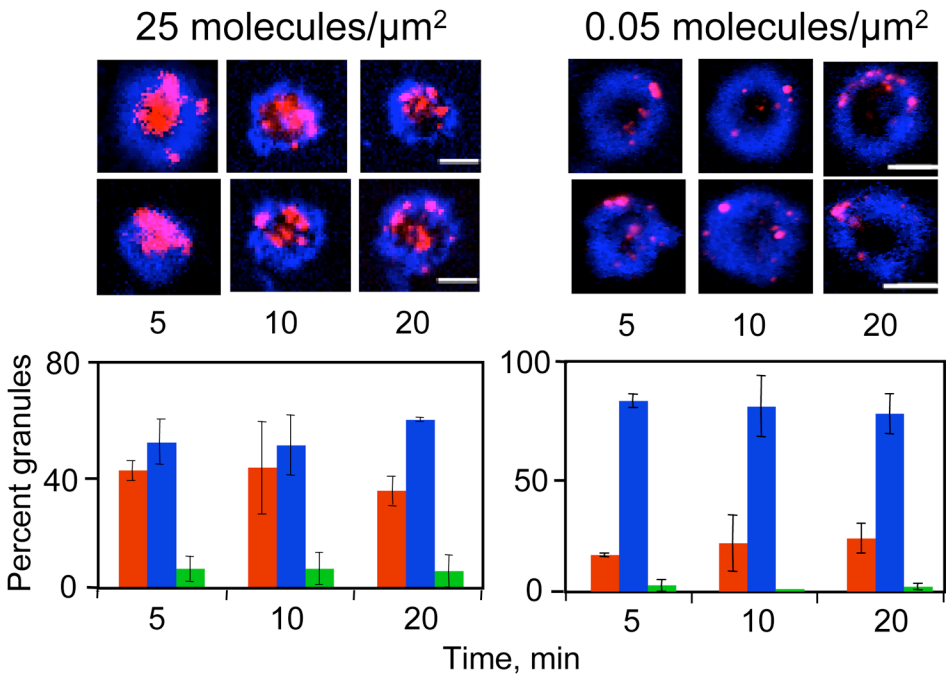

Figure S2. The density of pMHC on bilayers influences the ability of CTL to concentrate granules in the cSMAC

When the pMHC concentration on the bilayer surface was decreased to 0.05 molecules/μm^2 that yields approximately 2-5 pMHC molecules/cell, focusing of the granules in the cSMAC was not observed and the CD8$^+$ CTL demonstrated patterns of granule polarization similar to that in CD4$^+$ CTL. Top Panels: Representative images of two cells at each time point are shown for each concentration. ICAM-1 is blue and granules are red. Scale bar: 5μm. Bottom Panels: Images were taken at the designated times and then analyzed for the percent of granules in the cSMAC (red), pSMAC (blue), and pSMAC-cSMAC junction (green). Analysis was done on at least 15 cells from 2 independent experiments. Procedure: CD8$^+$ CTL (68A62) were exposed to bilayers containing the indicated concentrations of agonist pMHC (A2-IV9) and ICAM-1 (300 molecules/μm^2).

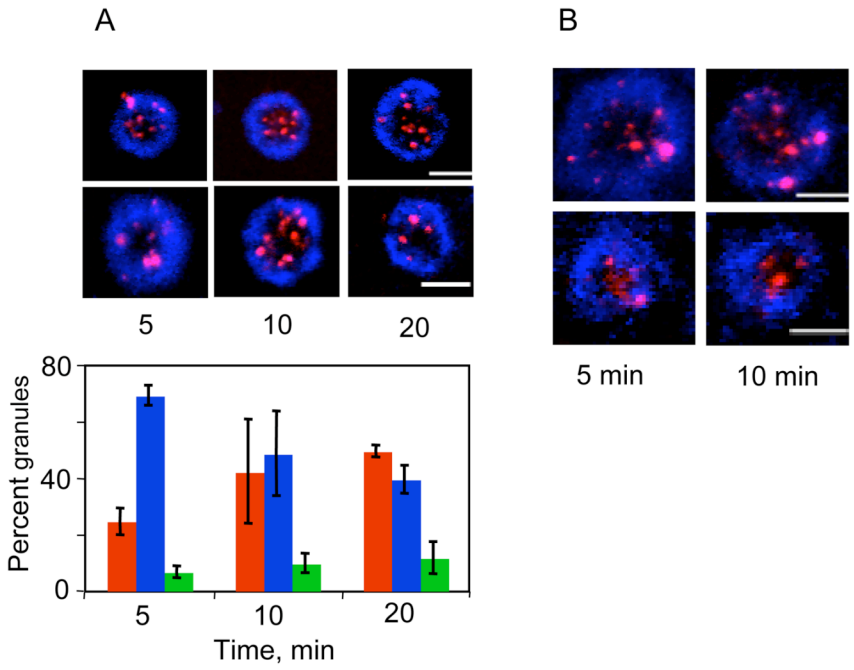

Figure S3. CD4$^+$ CTL are capable of concentrating granules in the cSMAC of the cytolytic synapse

(A) Strengthening of TCR stimulation in AC-25 CD4$^+$ CTL with anti-CD3 antibody incorporated into the lipid bilayer promoted recruitment of polarized granules to the center of the cytolytic synapse. Top panel: Representative images of CD4$^+$ CTL with ICAM-1 in blue and granules in red are shown. Scale bar: 5μm. Bottom panel: The percentage of granules localized in the pSMAC (blue), cSMAC (red), and pSMAC/cSMAC junction (green) is plotted at indicated time points. Procedure: AC-25 CD4$^+$ CTL were labeled with lysotracker and added to bilayers containing ICAM-1 (300 molecules/um^2) and anti-CD3 antibody (see Experimental Procedure) and images at the bilayer level were taken at the indicated times. At least 20 IS forming cells with significant lysotracker staining were analyzed for each time point in 2 independent experiments.

(B) Granule distribution in $CD8^+$ CTL stimulated with anti-CD3 containing bilayers is shown. $CD8^+$ CER43 CTL were exposed to bilayers with anti-CD3 and ICAM-1 as described above. Representative images of two cells are shown. ICAM-1 is blue and granules are red. The amount of granules observed in the cSMAC was similar to the amounts calculated for $CD4^+$ CTL (not shown). Scale bar: 5μm.

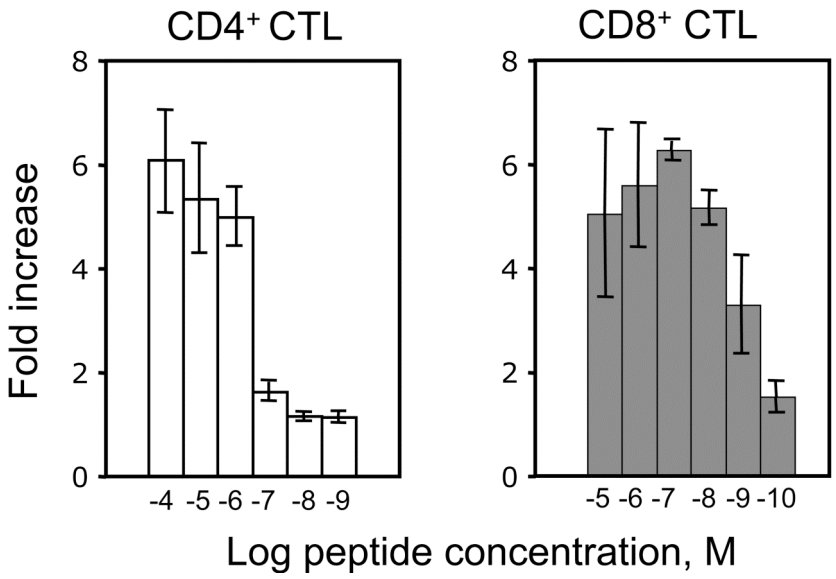

Figure S4. $CD4^+$ and $CD8^+$ CTL stimulated with live target cells show a different sensitivity in the Ca^{2+} response but reach a similar magnitude of Ca^{2+} flux

The dependence of the magnitude of Ca^{2+} flux in $CD4^+$ (left) and $CD8^+$ (right) CTL induced by live target cells sensitized with cognate peptides at different concentrations is shown. The results are from 3 independent experiments. Procedure: Fluo-3 labeled-CTL and unlabeled target cells were pre-warmed in a 37°C water bath then mixed together at a 1:1 ratio in a final 200 µl volume. The CTL:target mixture was centrifuged for 10s at a relative centrifugal force of 2,000 x *g* at room temperature in a microcentrifuge. The cell pellets were further incubated for 30 seconds and resuspended in 500 µl of pre-warmed assay media. The approximate time lapse from mixing to running the samples on the cytometer was about 1 minute. The samples were run on an Epics XL-MCL flow cytometer (Beckman Coulter). Intracellular calcium levels were determined using FlowJo software (Tree Star).

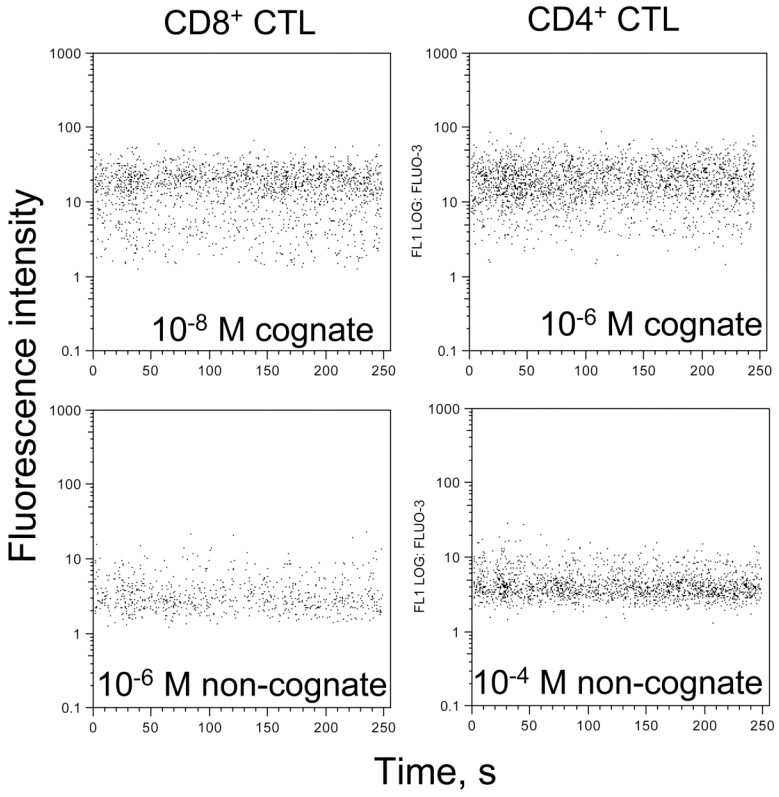

Figure S5. Ca^{2+} flux induced by live target cells in more ($CD8^+$) and less ($CD4^+$) effective CTL

Representative dot plots of Ca^{2+} flux in Fluo-3 labeled $CD4^+$ and $CD8^+$ CTL induced by live target cells sensitized with the respective cognate peptides. The plots show MFI over time. Top, Left: Representative dot plot of maximal increase in intracellular Ca^{2+} in CER43 $CD8^+$ CTL conjugated with target cells sensitized at 10^{-8} M cognate peptide concentration. Bottom, Left: Representative dot plot of baseline Fluo-3 fluorescence in $CD8^+$ CTL. Baseline was determined by the MFI when CTL were combined with target cells sensitized with non-cognate peptide at 10^{-6} M concentration. Top, Right: Representative dot plot of maximal Fluo-3 fluorescence in $CD4^+$ AC-25 CTL conjugated with target cells sensitized with 10^{-6} M concentration of cognate peptide. Bottom, Right:

Representative dot plot of baseline Fluo-3 fluorescence in $CD4^+$ CTL combined with target cells sensitized with non-cognate peptide at 10^{-4} M concentration.

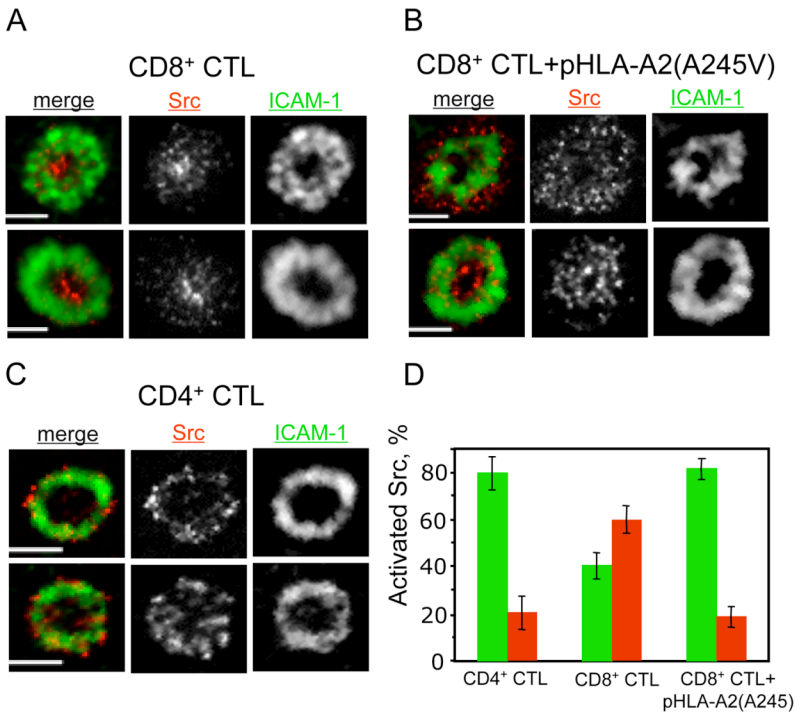

Figure S6. The amount of activated Src kinases in the cSMAC of CTL exercising either strong or weak cytolytic responses after 10 min exposure to lipid bilayers containing cognate pMHC with different potencies

Representative TIRF images of CER43 $CD8^+$ CTL interacting with bilayers containing ICAM-1 and either intact or mutated HLA-A2(A245V) loaded with cognate peptide are shown in panels (**A**) and (**B**), respectively. (**C**) Representative TIRF images of AC25 $CD4^+$ CTL contacting the bilayers with cognate pHLA-DR1 proteins and ICAM-1 are shown in panel. ICAM-1 is green, and phospho-Src is red. Scale bar: 5μm. (**D**) The percentage of the activated Src kinase fluorescence signal in the pSMAC (green) and the cSMAC (red) is depicted as a bar diagram. The data is from analysis of at least 70 IS-forming cells from 2 independent experiments. Procedure: CTL were exposed for 10 minutes to bilayers containing 500 molecules/μm^2 of cognate pMHC and 300

molecules/μm^2 of ICAM-1. Cells were then fixed, stained, and imaged to detect activated Src family kinases (phospho-Src) using TIRF microscopy.

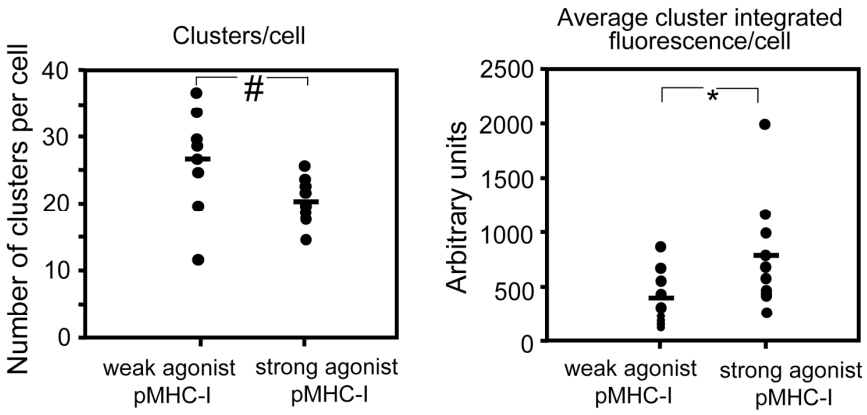

Figure S7. CD8$^+$ CTL recognizing strong agonist ligand recruit more activated Src kinases per clusters as opposed to the same CTL stimulated with weak agonist ligand

Comparison of the amount of activated Src kinases per cluster in 68A62 CD8$^+$ CTL exposed to bilayers containing either strong agonist IV9-HLA-A2 (25 molecules/μm^2) or weak agonist IV9-A7-HLA-A2 (500 molecules/μm^2) plus ICAM-1 (300 molecules/μm^2) is shown. The number of clusters per cell was measured as described in the Experimental Procedures and the results are presented in the left panel. The integrated fluorescence (arbitrary units) of each signaling cluster was measured and the average integrated fluorescence per cluster in each cell was calculated and depicted in the right panel. Data shown is from at least 10 IS-forming cells for each category. Statistical analysis was performed by Student's *t*-tests for paired data. #: $P < 0.02$, *: $P<0.05$. Procedure: CTL were exposed for 5 minutes to bilayers. Cells were then fixed and stained for activated Src family kinases (phospho-Src) as described in the Experimental Procedures. Activated Src kinases at the interface were imaged using TIRF microscopy.

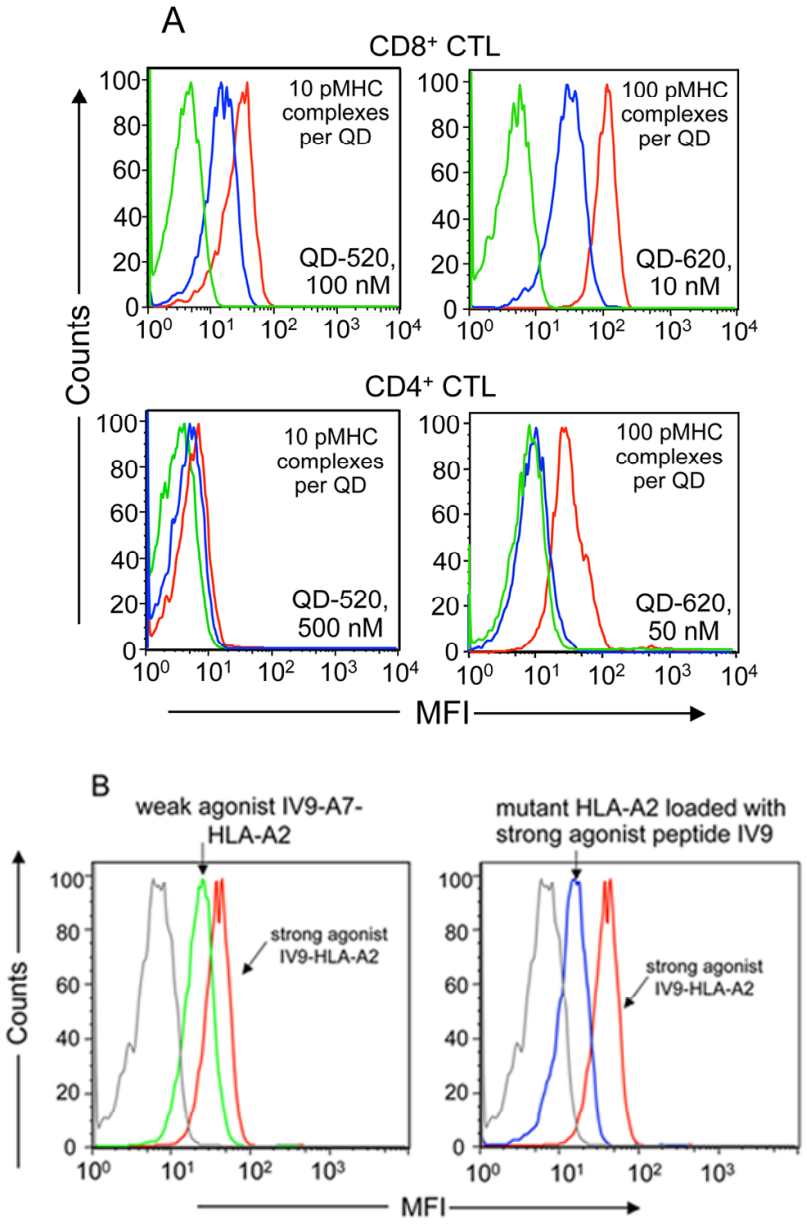

Figure S8. Binding of QD bearing pMHC ligands with various biological activities to cognate CTL

(**A**) Top: The binding of cognate complexes (red histograms, QD/GL9-HLA-A2) to CER43 $CD8^+$ CTL was detectable with both larger and smaller sized QD/pMHC conjugates. Binding of non-cognate QD/IV9-HLA-A2- conjugates was also evident (blue

histograms) and appeared to be CD8-dependent (not shown) as previously described (Anikeeva et al., 2006). QDs carrying mutated HLA-A2(A245V) loaded with non-cognate peptide were used as a negative control (green histograms). Bottom: Specific binding of smaller sized QD-520/pMHC cognate conjugates to AC-25 $CD4^+$ CTL was barely detectable despite staining at 37^0C (left). The specific binding of cognate QD/PP16-DRB1 conjugates (red histograms) to $CD4^+$ CTL was measurable when larger sized lipid-encapsulated QD-620 conjugates (Anikeeva et al., 2009) were used (right). Binding of non-cognate QD/A2-DRB1 conjugates (blue histograms) was only slightly above background staining by QD conjugated with an irrelevant QD/GL9-HLA-A2 protein (green histograms). Procedure: QD/pMHC conjugates were assembled according to previously published procedure (Anikeeva et al., 2006; Anikeeva et al., 2009). CER43 $CD8^+$ CTL were stained with QD/pMHC conjugates at room temperature for 30 min. AC-25 $CD4^+$ CTL were stained with QD/pMHC conjugates for 30 min at either 37^oC (left) or room temperature (right). After washing the CTL were analyzed on an Epics XL-MCL flow cytometer (Beckman Coulter).

(**B**) QD/pMHC conjugates containing either mutant HLA-A2(A245V) loaded with cognate peptide or intact HLA-A2 loaded with weak agonist peptide show decreased ability to bind to the surface of $CD8^+$ CTL. 68A62 $CD8^+$ CTL were stained with 10 nM DHLA-capped QD-620 bearing strong agonist IV9-HLA-A2 (red histograms), weak agonist IV9-A7-HLA-A2 (green histogram), mutant HLA-A2(A245V) loaded with IV9 (blue histogram), or irrelevant pMHC-II complexes (grey histograms). The ratio of pMHC-to-QD-620 was kept at 40 in all experiments. The decrease of MFI indicates a weaker binding of QD/pMHC conjugates.

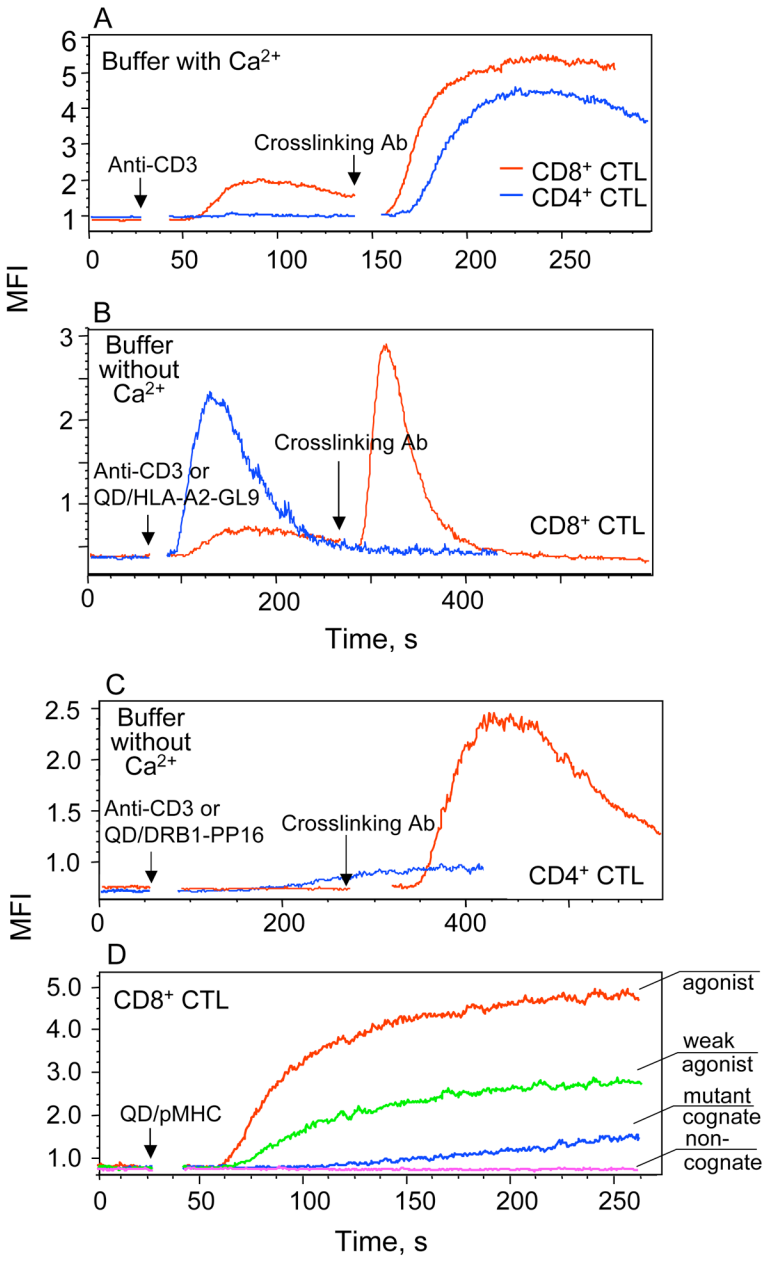

Figure S9. Calcium flux in CD8⁺ and CD4⁺ CTL induced by QD/pMHC conjugates and anti-CD3 antibodies

(**A**) Comparison of Ca^{2+} flux induced by cross-linked anti-CD3 mAb in $CD4^+$ AC-25 and $CD8^+$ CER43 CTL labeled with Fluo-3. (**B**) 1.5 nM of lipid encapsulated QD-620/ GL9-HLA-A2 conjugates (blue) or anti-CD3 mAb (10 μg/ml) cross-linked with horse anti-

mouse antibodies (red) from Vector Laboratories were added to CER-43 $CD8^+$ CTL labeled with Fluo-3. (**C**) 20 nM of lipid encapsulated QD-620/PP16-DRB1 conjugates (blue) or anti-CD3 antibody (10 μg/ml) cross-linked with horse anti-mouse antibodies (red) were added to AC-25 $CD4^+$ CTL labeled with Fluo-3. Calcium response was induced in the presence (**A**) or absence (**B and C**) of calcium in the extracellular medium. To remove residual Ca^{2+} from the assay buffer EGTA was added to the final concentration of 1 mM. (**D**) Variations in Ca^{2+} influx by 68A62 $CD8^+$ CTL induced by 2 nM DHLA-capped QD-620 loaded with weak agonist (IV9-A7-HLA-A2), strong agonist (IV9-HLA-A2), mutant cognate (IV9-HLA-A2(A245V)), or control non-cognate (GL9-HLA-A2) pMHC complexes. The experiments were performed in the presence of extracellular calcium. The number of pMHC complexes per dot was fixed at 40. Calcium flux was measured in Fluo-3 (λ_{max} = 526 nm) labeled CTL to avoid interference with the fluorescence of QD-620 (λ_{max} = 620 nm). Representative results are shown.

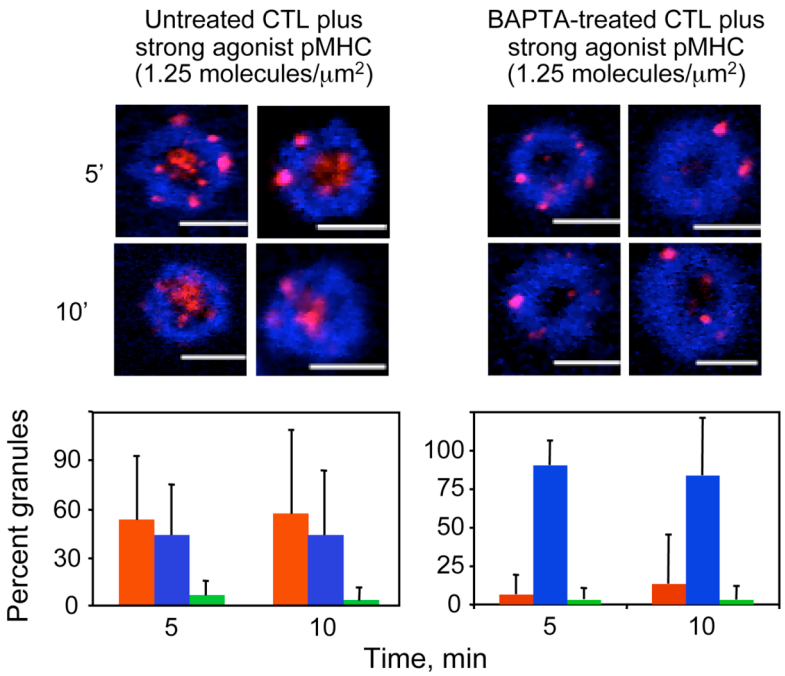

Figure S10. Figure S10. BAPTA treatment decreases the ability of 68A62 CD8$^+$ CTL exposed to bilayers containing a low density of strong agonist IV9-HLA-A2 ligand to concentrate cytolytic granules in the cSMAC

Top panel: Representative images of BAPTA-treated (right) or untreated (left) 68A62 CTL interacting with bilayers containing 1.25 molecules/μm^2 of strong agonist IV9-HLA-A2 are presented. ICAM-1 is blue and granules are red. Scale bar: 5μm.

Bottom panel: The percentage of granules localized in the pSMAC (blue bars), cSMAC (red bars), and pSMAC/cSMAC junction (green bars) at the bilayer level is depicted. At least 10 IS forming cells were analyzed for each category in 2 independent experiments.

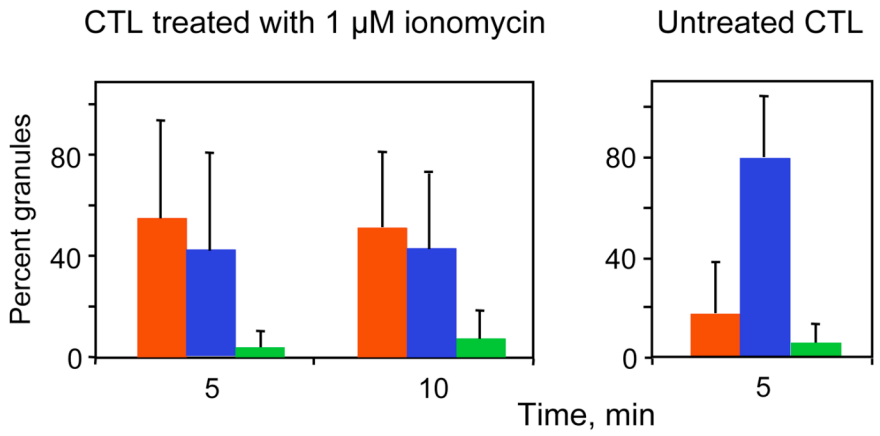

Figure S11. Ionomycin treatment of 68A62 CD8$^+$ CTL stimulated with bilayers containing a weak agonist IV9-A7-HLA-A2 enhances the CTL ability to concentrate granules in the cSMAC of the cytolytic synapses.

68A62 CD8$^+$ CTL were exposed to ICAM-1-containing bilayers modified with IV9-A7-HLA-A2 weak agonist at 1 μM plus 1 μM ionomycin as described in **Figure 4D**. The percentage of granules localized in the pSMAC (blue bars), cSMAC (red bars), and pSMAC/cSMAC junction (green bars) at the bilayer level was determined as in Experimental Procedures.

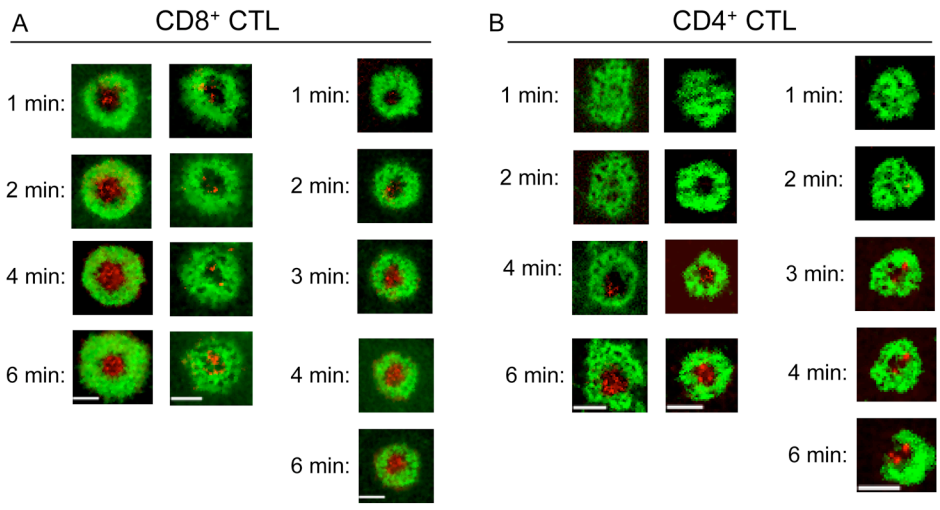

Figure S12. Direct visualization of granule release by $CD8^+$ and $CD4^+$ CTL

CTL and fluorescent-labeled anti-CD107a Fab (10μg/ml) were injected into flow cells as described in **Figure 6**. Images were then taken at one-minute intervals to monitor granule release by the appearance of CD107a on the CTL membrane. Multiple representative images of CER43 $CD8^+$ CTL (A) and AC-25 $CD4^+$ CTL (B) are shown. ICAM-1 is green and CD107a is red. Scale bar: 5 μm.

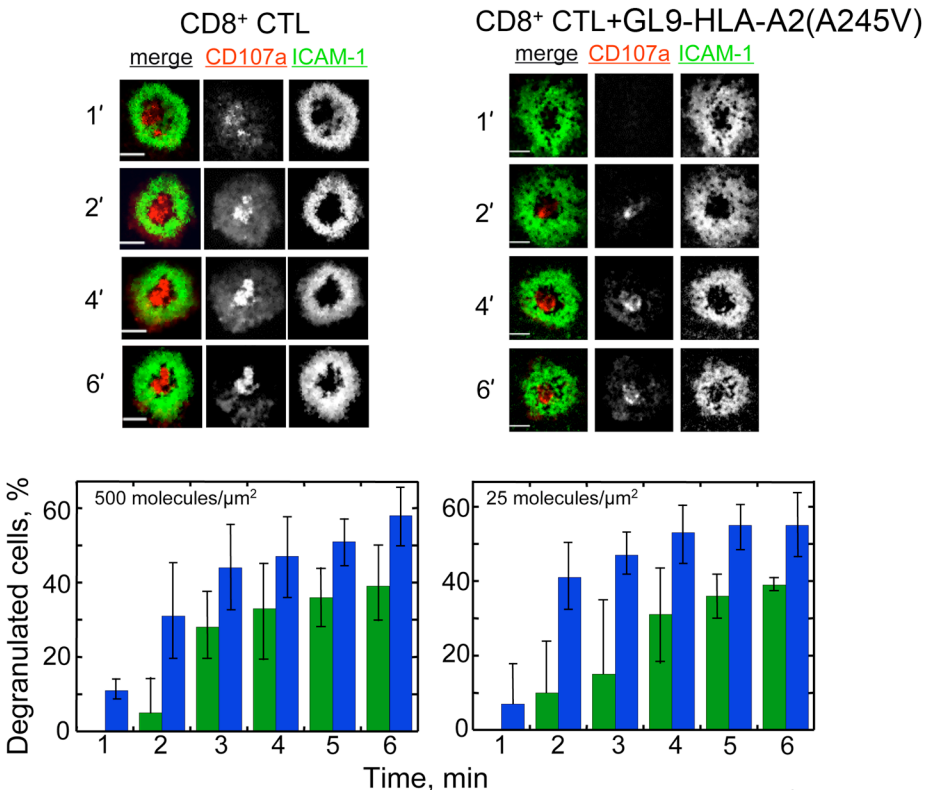

Figure S13. Kinetics of granule release by CD8⁺ CTL interacting with bilayers containing either intact or mutated HLA-A2(A245V) loaded with the same cognate peptide

Representative images demonstrate the influence of the CD8-HLA-A2 interactions on the kinetics of granule release by CD8⁺ CER43 CTL (upper panels). The graphs (bottom panels) show the percentage of CD107a positive CTL interacting with bilayers containing ICAM-1 (300 molecules/μm^2) and cognate pMHC at a density of either 500 molecules/μm^2 (left) or 25 molecules/μm^2 as a function of time (right). The frequency of degranulating CD8$^+$ CTL exposed to either GL9-HLA-A2 (blue) or GL9-HLA-A2(A245V) (green) molecules in the bilayers at different time-points is shown (bottom panels). More than 30 cells from 3 independent experiments were analyzed at the pMHC

density of 500 molecules/μm^2 and more than 20 cells from 2 independent experiments were analyzed at the pMHC density of 25 molecules/μm^2.

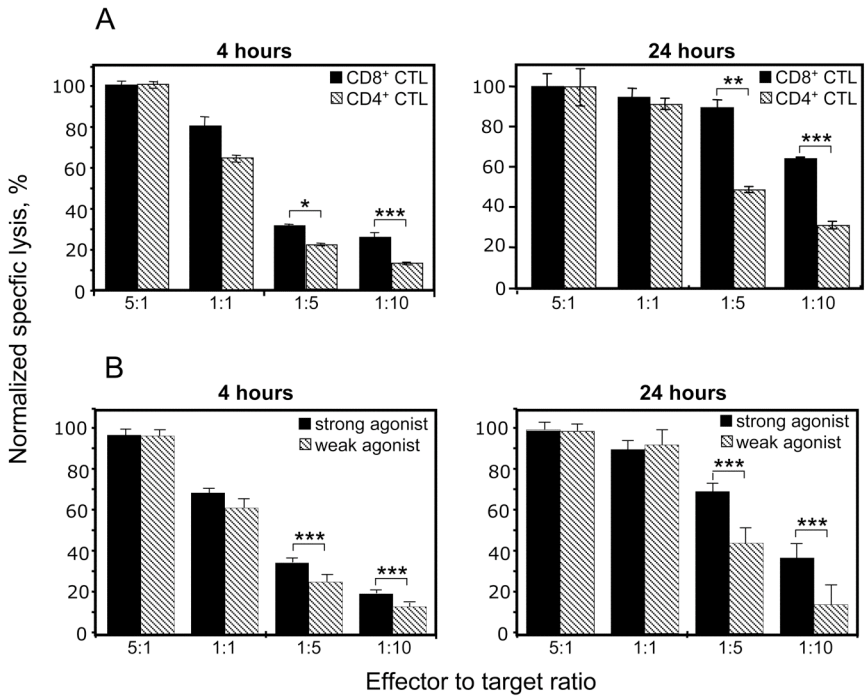

Figure S14. Difference in the kinetics of target cell lysis by more and less effective CTL

(**A**) Changes in specific lysis of T2-DR1 target cells by human CER43 $CD8^+$ CTL and AC-25 $CD4^+$ CTL at different effector-to-target ratio during 4 (left) or 24 hours (right). The E:T ratio was titrated to determine the efficiency of lysis at various time when CTL numbers are limiting. The target cells were sensitized with peptide concentrations required to reach maximal specific lysis by $CD4^+$ (10^{-5} M) and $CD8^+$ (10^{-8} M) CTL in a standard 4-hour assay; both CTL release similar amount of granules with equal potency at these conditions (Beal et al., 2008). The results were normalized to the specific lysis at 5:1 E:T ratio. Statistical analysis was performed by Student's *t*-tests for paired data. *: P<0.02, **: P<0.01 and ***P<0.005

(**B**) T2-DR1 cells were sensitized with either strong agonist (IV9) or weak agonist (A4-IV9) peptides at 10^{-8} M or 10^{-6} M concentrations, respectively, and were incubated with 68A62 $CD8^+$ CTL at various effector-to-target ratios (as indicated). At these conditions CTL released similar amount of granules (data not shown). The percent specific lysis of the target cells was determined after 4 (left) and 24 (right) hours incubation. Results of representative experiments are shown and statistical analysis was performed using Student's *t*-tests. ***: $P<0.005$

Procedure: For effector-to-target (E:T) ratios greater than 1:1, $5x10^3$ target cells were ^{51}Cr-labeled and then sensitized for one hour with various amounts of peptide in 150 μl R10 (RPMI-1640 containing 10% FCS). CTL in 50 μl of complete R10 were then added. For E:T ratios less than 1:1, the number of ^{51}Cr-labeled target cells was varied accordingly while the effector cell number remained constant at $5x10^3$ CTL. The assays were performed in 96-well round-bottomed plates at indicated E:T ratios. The plates were incubated for the various times in a CO_2 incubator at 37^0C and ^{51}Cr release was measured in 100 μl of supernatant from each well. Percent specific lysis was determined as previously described (Sykulev et al., 1996).

Movie Legend. Degranulation of $CD8^+$ and $CD4^+$ CTL in real-time

CTL were combined with fluorescent-labeled anti-CD107a Fab fragments and were added to lipid bilayers containing ICAM-1 (300 molecules/um^2) and cognate pMHC (500 molecules/um^2) as described in Experimental Procedures. The interface was imaged using TIRF microscopy. Images were obtained at 1-minute intervals and rebuilt at 1 frame per second for a total of 6 frames. More effective CER43 $CD8^+$ CTL rapidly released granules that were seen 1 minute after the CTL adhered to the bilayer (Movie#1). In contrast, granule release by less effective AC25 $CD4^+$ CTL was not observed until 3 minutes after the CTL adhered to the bilayer (Movie #2). Time zero in each case was set immediately after the cells began to adhere to the bilayers as was evident from observed IRM images. The TIRF images and ICAM-1 images were then sequentially taken at every minute.

Supplemental References

Anikeeva, N., Lebedeva, T., Clapp, A.R., Goldman, E.R., Dustin, M.L., Mattoussi, H., and Sykulev, Y. (2006). Quantum dot/peptide-MHC biosensors reveal strong CD8-dependent cooperation between self and viral antigens that augment the T cell response. Proc Natl Acad Sci U S A *103*, 16846-16851.

Anikeeva, N., Mareeva, T., Liu, W., and Sykulev, Y. (2009). Can oligomeric T-cell receptor be used as a tool to detect viral peptide epitopes on infected cells? Clin Immunol *130*, 98-109.

Anikeeva, N., Somersalo, K., Sims, T.N., Thomas, V.K., Dustin, M.L., and Sykulev, Y. (2005). Distinct role of lymphocyte function-associated antigen-1 in mediating effective cytolytic activity by cytotoxic T lymphocytes. Proc Natl Acad Sci U S A *102*, 6437-6442.

Beal, A.M., Anikeeva, N., Varma, R., Cameron, T.O., Norris, P.J., Dustin, M.L., and Sykulev, Y. (2008). Protein kinase Ctheta regulates stability of the peripheral adhesion ring junction and contributes to the sensitivity of target cell lysis by CTL. J Immunol *181*, 4815-4824.

Sykulev, Y., Joo, M., Vturina, I., Tsomides, T.J., and Eisen, H.N. (1996). Evidence that a single peptide-MHC complex on a target cell can elicit a cytolytic T cell response. Immunity *4*, 565-571.